Mechanically switchable photonic crystal filter with either all-pass transmission or flat-top reflection characteristics

Wonjoo Suh and Shanhui Fan

Department of Electrical Engineering, Stanford University, Stanford, California 94305

Received April 17, 2003

We theoretically introduce a new type of optical all-pass filter based on guided resonance in coupled photonic crystal slabs. The filter exhibits near-complete transmission for both on- and off-resonant frequencies and yet generates large resonant group delay. We further show that such a filter can be mechanically switched into a flat-top band rejection filter. © 2003 Optical Society of America

OCIS codes: 230.5750, 260.5740, 230.3990, 120.2440.

Optical filters play important roles in communication systems. In particular, a narrowband flat-top reflection filter, which reflects a particular wavelength channel while letting other channels pass through, is needed to achieve the wavelength sensitivity in wavelength-division multiplexing systems.[1] On the other hand, an all-pass transmission filter, which generates significant delay at resonance, while maintaining 100% transmission both on and off resonance, is useful for applications such as optical delay or dispersion compensation.[2]

In this Letter we introduce a mechanically switchable photonic crystal filter structure that can function as either a flat-top reflection filter or an all-pass transmission filter. The structure, shown in Fig. 1, consists of two photonic crystal slabs. Each slab is constructed by introduction of a periodic array of air holes into a high-index guiding layer. We show that for normally incident light one can switch the transmission characteristic of the structure by simply varying the distance between the slabs. Furthermore, unlike all previously reported all-pass reflection filters based on Gires–Tournois interferometers,[3] which use multiple dielectric stacks, our structure generates an all-pass transmission spectrum, which significantly simplifies signal extraction and optical alignment. In addition, the spectral response is polarization independent because of the 90° rotational symmetry of the structure.

The filter function of our device relies on the guided resonance phenomenon in each photonic crystal slab. Guided resonance is a class of optical mode that is strongly confined by the dielectric slab and yet can couple into radiation modes because of the phase-matching mechanism provided by the periodic index contrast.[4,5] As light is normally incident upon the slab, the wave can pass through the slab either directly or indirectly by first exciting the resonance and then decaying out. In the particular case where the partial transmission coefficient through the direct pathway is unity, the reflection from the crystal exhibits a Lorentzian line shape with 100% reflectivity at the resonant frequency,[6] as can be seen in Fig. 2 for the transmission through a single slab[7] with a dielectric constant of 11.4 [which is appropriate for GaAs at 1.55 μm (Ref. 8)], a thickness of $1.05a$ and a radius of $0.1a$ for the air holes (a is the lattice constant).

Having two slabs creates additional flexibility with which to engineer spectral functions.[9] Let us first consider an all-pass transmission filter for optical delay applications. A single resonance can generate significant optical delay. However, in the single-slab geometry shown in Fig. 2, since the reflected amplitude comes entirely from the resonant decay, there is a strong variation of the transmitted intensity as a function of frequency.

To achieve an all-pass characteristic with no intensity variation over the resonance bandwidth, it is therefore necessary to use at least two resonances. For simplicity, we consider a system with two identical slabs, as shown in Fig. 1. Each slab supports a single resonance within the bandwidth of interest. Since there is mirror symmetry parallel to the slab, the resonant modes of the coupled system can be decomposed into either even or odd modes with respect to the mirror plane. When external light is incident upon the slabs, both the even and odd modes are excited. The power in each resonance then decays in both forward and backward directions. Since the two modes have different symmetry, the decaying amplitudes in the backward direction acquire an opposite phase and interfere destructively. Therefore, complete transmission over the bandwidth of interest becomes possible, provided that the even and odd modes possess the same resonant frequency and the same width.[10] To achieve complete transmission we

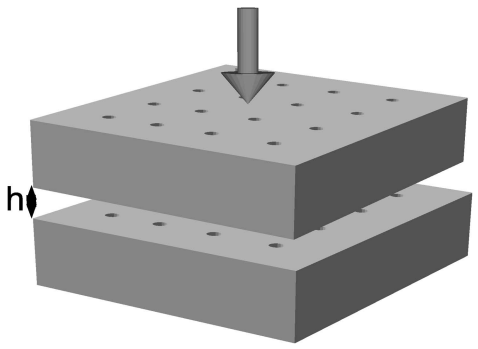

Fig. 1. Schematic of a mechanically tunable photonic crystal filter consisting of two photonic crystal slabs. The arrow represents the direction of the incident light. The spectral response function of the filter is tunable by varying the distances between the two slabs.

0146-9592/03/191763-03$15.00/0

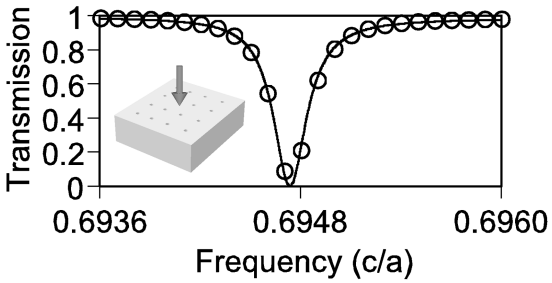

Fig. 2. Transmission spectrum through a single photonic crystal slab for normally incident light. The crystal structure shown in the inset consists of a square lattice of air holes of radius $0.1a$, where a is the lattice constant. The slab has a dielectric constant of 11.4 and a thickness of $1.05a$. The open circles are the numerical results from a FDTD simulation. The solid curve is from the analytical theory in Ref. 7.

place two slabs close to each other so that the modes in the two slabs can couple through an evanescent tunneling pathway, in addition to the free-space propagation of light between the slabs.

The idea described above can be quantified by use of the coupling of modes in a time-dependent formalism for optical resonators.[7,11] The theoretical model describes the dynamics of the optical resonance amplitudes a and b in the two slabs. For the structure in Fig. 2, which possesses a Lorentzian resonance, the dynamic equation for the amplitude a in the first slab is

$$\frac{da}{dt} = \left(j\omega_0 - \frac{1}{\tau}\right)a + j\sqrt{\frac{1}{\tau}}\,S_{1+} + j\sqrt{\frac{1}{\tau}}\,S_{2+} + j\kappa b\,, \tag{1}$$

$$S_{1-} = S_{2+} + j\sqrt{\frac{1}{\tau}}\,a\,, \qquad S_{2-} = S_{1+} + j\sqrt{\frac{1}{\tau}}\,a\,, \tag{2}$$

where ω_0 is the resonance frequency and τ is the resonance lifetime. S_{1+}, S_{2+}, S_{1-}, and S_{2-} are incoming and outgoing waves from either side of the first slab. The coupling constant κ describes the strength of evanescent tunneling between the two slabs and is real because of energy conservation and mirror symmetry constraints. Similarly, the equations for the amplitude b in the second slab can be written as

$$\frac{db}{dt} = \left(j\omega_0 - \frac{1}{\tau}\right)b + j\sqrt{\frac{1}{\tau}}\,P_{1+} + j\sqrt{\frac{1}{\tau}}\,P_{2+} + j\kappa a\,, \tag{3}$$

$$P_{1-} = P_{2+} + j\sqrt{\frac{1}{\tau}}\,b\,, \qquad P_{2-} = P_{1+} + j\sqrt{\frac{1}{\tau}}\,b\,, \tag{4}$$

where P_{1+}, P_{2+}, P_{1-}, and P_{2-} are incoming and outgoing waves from either side of the second slab. Also, since the wave can propagate between the slabs, we have

$$P_{1+} = \exp(-j\phi)S_{2-}\,, \qquad P_{1-} = \exp(j\phi)S_{2+}\,, \tag{5}$$

where $\phi = (\omega/c)h$ and h is the distance between the edges of the slabs. Using Eqs. (1)–(5), we can eliminate wave amplitudes that are propagating between the slabs to arrive at the dynamic equations for the even resonance, A $(=a + b)$, and the odd resonance, B $(=a - b)$. Then, when the coupling coefficient is set to be $\kappa = -j\exp(-j\phi)/\tau$, and when $\phi = \pi/2$ is chosen, the even and odd resonances will possess the same resonance frequency and decay length. Under these circumstances, the transmission coefficient becomes

$$t = \exp(-j\phi)\,\frac{j(\omega - \omega_0) - 1/\tau}{j(\omega - \omega_0) + 1/\tau}\,, \tag{6}$$

and, indeed, the structure behaves as an all-pass filter.

As a physical realization of the theoretical analysis, we consider the two-slab structure, each slab of which is shown in Fig. 2, with a resonance frequency at 0.694 (c/a). In a FDTD simulation,[5,12,13] the line shapes of the even and odd modes can be obtained by Fourier transformation of the temporal decay of the resonance amplitude. When the displacement between the slabs is chosen to be $0.4a$, the resonant line shapes of the even and odd modes overlap almost completely [Fig. 3(a)]. For such a structure, the transmission spectrum indeed shows near 100% transmission over the entire bandwidth both on and off resonance [Fig. 3(b)], and yet a large resonant delay is generated in the vicinity of the resonant frequency [Fig. 3(c)]. To compare the simulation with the theory, we extract the parameter from Fig. 3(a), and generate the theoretical spectra by use of Eqs. (1)–(5). The simulations show excellent agreement with the analytic theory.

The spectral response function of the two-slab structure can be tuned by mechanical variation of the distance between the slabs. As we increase the

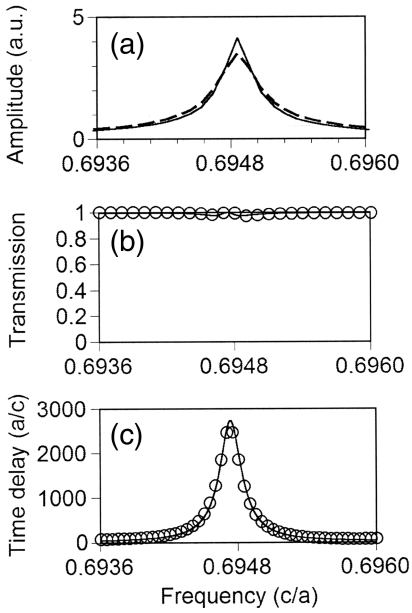

Fig. 3. Spectral response functions for the two-slab structure shown in Fig. 1, with an edge-to-edge distance of $0.4a$. (a) Resonance amplitudes of the even mode (dashed curve) and the odd mode (solid curve). (b) Transmission spectrum for normally incident light. (c) Group delay. In both (b) and (c), the solid curve represents the theory and the open circles correspond to FDTD simulations.

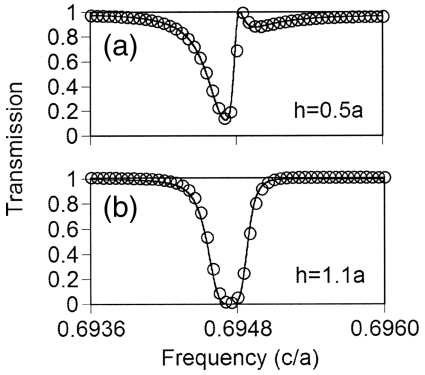

Fig. 4. Transmission spectra through the two-slab structure shown in Fig. 1 as we vary the distance between the slabs to be (a) $0.5a$, (b) $1.1a$. The solid curves represent the theory, and the open circles correspond to FDTD simulations.

distance between the slabs, the evanescent coupling becomes negligible, and it is no longer possible to generate all-pass transmission. Rather, significant reflection occurs in the vicinity of the resonance [Fig. 4(a)]. In particular, by choosing $h = 1.1a$, one could generate a flat-top reflection spectrum,[14] as demonstrated by FDTD simulations in Fig. 4(b). Thus, with mechanical tuning, a guided resonance device can generate two types of filter response that are useful for optical communication systems. In addition, the flat spatial dispersion of the guided resonance may permit operation of such filters with a large range of operation angles.

This work was partially supported by the U.S. Army Research Laboratories under contract DAAD17-02-C-0101 and by National Science Foundation (NSF) grant ECS-0200445. The computational time was provided by the NSF National Resource Allocation Committee program. We thank Mehmet Fatih Yanik for developing the software code used in this work. S. Fan's e-mail address is shanhui@stanford.edu.

References

1. D. K. Jacob, S. C. Dunn, and M. G. Moharam, Appl. Opt. **41,** 1241 (2002).
2. C. K. Madsen, J. A. Walker, J. E. Ford, K. W. Goossen, T. N. Nielsen, and G. Lenz, IEEE Photon. Technol. Lett. **12,** 651 (2000).
3. F. Gires and P. Tournois, C. R. Hebd. Seances Acad. Sci. B Sci. Phys. (France) **268,** 313 (1969).
4. M. Kanskar, P. Paddon, V. Pacradouni, R. Morin, A. Busch, J. F. Young, S. R. Johnson, J. Mackenzie, and T. Tiedje, Appl. Phys. Lett. **70,** 1438 (1997).
5. S. Fan and J. D. Joannopoulos, Phys. Rev. B **65,** 235112 (2002).
6. R. Magnusson and S. S. Wang, Appl. Phys. Lett. **61,** 1022 (1992).
7. S. Fan, W. Suh, and J. D. Joannopoulos, J. Opt. Soc. Am. A **20,** 569 (2003).
8. E. D. Palik, *Handbook of Optical Constants of Solids* (Academic, San Diego, Calif., 1985), p. 439.
9. W. Suh, M. F. Yanik, O. Solgaard, and S. Fan, Appl. Phys. Lett. **82,** 1999 (2003).
10. S. Fan, P. R. Villeneuve, J. D. Joannopoulos, and H. A. Haus, Phys. Rev. Lett. **80,** 960 (1998).
11. H. A. Haus, *Waves and Fields in Optoelectronics* (Prentice-Hall, Englewood Cliffs, N.J., 1984).
12. K. S. Kunz and R. J. Luebbers, *The Finite-Difference Time-Domain Methods for Electromagnetics* (CRC, Boca Raton, Fla., 1993).
13. A. Taflove and S. Hagness, *Computational Electrodynamics: The Finite-Difference Time-Domain Methods* (Artech House, Boston, Mass., 2000).
14. Similar flat-top behavior in one-dimensional grating structures was reported in Ref. 1.